



Self-Focusing and the Talbot Effect in Conformal Transformation Optics

Xiangyang Wang,¹ Huanyang Chen,^{2,*} Hui Liu,^{1,†} Lin Xu,² Chong Sheng,¹ and Shining Zhu¹

¹National Laboratory of Solid State Microstructures and School of Physics,

Collaborative Innovation Center of Advanced Microstructures, Nanjing University, Nanjing, Jiangsu 210093, China

²Institute of Electromagnetics and Acoustics and Department of Electronic Science, Xiamen University, Xiamen 361005, China

(Received 27 February 2017; published 18 July 2017)

Transformation optics has been used to propose various novel optical devices. With the help of metamaterials, several intriguing designs, such as invisibility cloaks, have been implemented. However, as the basic units should be much smaller than the working wavelengths to achieve the effective material parameters, and the sizes of devices should be much larger than the wavelengths of illumination to work within the light-ray approximation, it is a big challenge to implement an experimental system that works simultaneously for both geometric optics and wave optics. In this Letter, by using a gradient-index microstructured optical waveguide, we realize a device of conformal transformation optics (CTO) and demonstrate its self-focusing property for geometry optics and the Talbot effect for wave optics. In addition, the Talbot effect in such a system has a potential application to transfer digital information without diffraction. Our findings demonstrate the photon controlling ability of CTO in a feasible experiment system.

DOI: 10.1103/PhysRevLett.119.033902

In gravitational lensing [1], light rays are bent by a star because its gravitation changes the geometric property of space. Similarly, the propagation direction of light is altered in a transmitting medium relative to a vacuum because of the interaction between the electromagnetic field and matter [2]. Based on an analogy between spacetime geometry and light propagation in a medium, two papers on invisibility cloaks [3,4] started research into transformation optics (TO) [5–7], which deepened our understanding of gravitational analogues in optical systems. Furthermore, general relativity in electrical engineering (an analogue electromagnetic system) has been proposed [8–10] and implemented at visible frequencies [11–14].

In the last decade, developments in material science have enhanced our ability to design optical devices [6] and control electromagnetic waves using TO. Moreover, the principles of transformation optics can be harnessed to control other kinds of wave [15–18]. Although TO is a very beautiful theory and has many fantastic applications, it has encountered some difficulties in experiments. In the earlier work on invisibility cloaking [3,19], different kinds of split-ring resonance structures are used to tune the effective material parameters, which are inhomogeneous and anisotropic tensors. The working wavelengths should be much larger than the resonance units. On the other hand, in order to satisfy the light-ray approximation, the working wavelengths should be much smaller than the sizes of devices. For this reason, it is a great challenge to experimentally realize both geometric optics and wave optics in a single transformation-optical device [20]. In geometric optics, light is treated as particles, and the only important thing is the trajectories. But in wave optics not only do the trajectories matter, but also phase changes play a very important role.

In two-dimensional space, conformal transformation optics (CTO) [4,21], as a branch of TO, can steer light rays by using a dielectric medium with an inhomogeneous and isotropic refractive index profile. Light rays (in the geometric-optics regime) can be bent by such a dielectric medium. Recently, conformal transformation optics was further expanded into the realm of wave optics, and many groups have done extensive studies in this field, such as cloaking [22–26], whispering gallery modes [27], broadband plasmonic devices [28,29], the Casimir effect [30], and analysis of electron energy loss [31]. So devices from CTO might be good candidates for working simultaneously in the geometric-optics and wave-optics regimes.

In this Letter we introduce a conformal lens, also known as the Mikaelian lens [32]. This conformal lens is mapped from the Maxwell's fish-eye lens by an exponential conformal mapping [33]. We construct such a conformal lens with a gradient-index microstructured optical waveguide and observe that it can self-focus a beam: a geometric-optics property. Moreover, we see the Talbot effect in the same lens, which stems from a phase change and only happens for wave optics.

The Talbot effect was first discovered in 1836 [34] and was explained by Rayleigh in 1881 [35]. It was rediscovered at the beginning of the 20th century [36–38], and in the mid-1950s Cowley and Moodie revisited this effect [39,40], which received much attention [41–44]. Recently the Talbot effect has been realized in several different systems, such as metamaterials [45] and surface plasmonics [46], which have many applications [47,48]. By proper design, we find that the Talbot effect in the conformal lens can be further applied to transfer digital information without diffraction. We verified these conformal Talbot effects through

experiment measurements, numerical simulation, and analytic calculations.

Let us first recall the basic principle of CTO [4,21]. In a two-dimensional space denoted by $w = u + vi$, if there is a refractive index profile $n_w(u + vi)$, light rays will propagate along curved trajectories if n_w is not uniform. Considering another space denoted by $z = x + yi$, related by a conformal mapping [$w = w(z)$] which satisfies Cauchy-Riemann condition [49], one can construct a point-to-point corresponding relationship between $u-v$ space and $x-y$ space. If the refractive index profile $n_w(u, v)$ in $u-v$ space and $n_z(x, y)$ in $x-y$ space satisfy [4]

$$n_z = \left| \frac{dw}{dz} \right| n_w, \quad (1)$$

then light trajectories in $x-y$ space can be simply obtained by conformal mapping from those in $u-v$ space according to CTO (see Supplemental Material Sec. I for more details [50]). Therefore, Eq. (1) establishes the corresponding relationship of light propagation between two spaces by conformal mapping.

Now we introduce a CTO device that starts from the well-known Maxwell's fish-eye lens in two dimensions. Its refractive index profile is $n_w(u, v) = 2\alpha/(1 + u^2 + v^2)$, where 2α is the refractive index at the center [Fig. 1(a)]. By using the variational method to obtain light trajectories [54], we know that all the light rays emitted from a point source at point **A** will travel along the solid red circles and converge to an image at point **B**. Suppose we have an exponential conformal mapping $w = \exp(\beta z)$, which can map a $u-v$ complex plane in Fig. 1(a) to a ribbonlike region

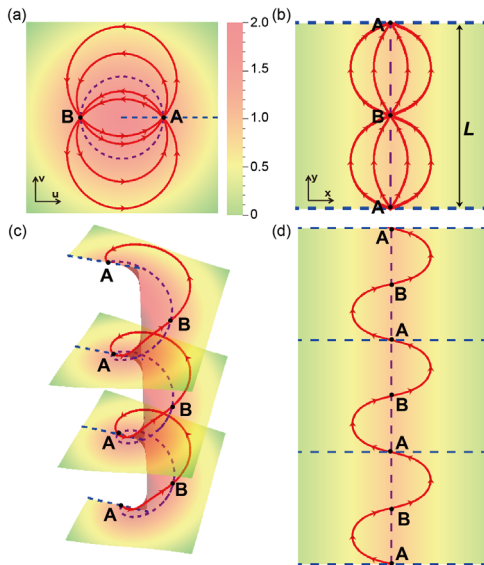


FIG. 1. Exponential conformal mapping. (a) Imaging by Maxwell-fish eye in $u-v$ space. (b) Self-focusing of light rays by Mikaelian lens in $x-y$ space. (c) A “spiral” light ray in the Riemann surfaces. (d) A sinelike ray in $x-y$ space.

of $x-y$ space in Fig. 1(b). The parameter β determines the width of the ribbonlike region. In Fig. 1(b), the two dashed blue lines are boundaries of the ribbonlike region, which are mapped from the branch cut (dashed blue line) in Fig. 1(a), with width $L = 2\pi/\beta$. According to Eq. (1), we can derive the refractive index profile in $x-y$ space in Fig. 1(b) as [33],

$$n_z = \frac{n_0}{\cosh(\beta x)}, \quad (2)$$

where $n_0 = \alpha\beta$. Here, if we choose $\alpha = 1$ and $\beta = 1$, the refractive-index profile is that shown on the left of Fig. 1(a). The refractive indices along the dashed purple lines in Fig. 1(a) and 1(b) are the same. Light rays (red curve with arrows) of Fig. 1(b) can be mapped from those of Fig. 1(a) by $w = e^{\beta z}$, which can also be obtained by the variational method of geometric optics. In fact, we can expand this lens in the y direction to construct a Mikaelian lens, where light rays can be self-focused [32] periodically along the line at $x = 0$, with a half of the periodicity L [Fig. 1(d)]. One can also imagine that the whole conformal lens in Fig. 1(d) is mapped from the Riemann surface of exponential conformal mapping shown in Fig. 1(c). The Riemann surface contains infinite numbers of Riemann sheets. Here we only show three of them, each of which is a complex plane endowed with a Maxwell's fish eye lens. They are connected by branch cuts shown as blue dashed lines in Fig. 1(c). Because of the existence of the inhomogeneous lens, a light ray (in red) will travel along a circle. Once it passes through the branch cut, it will go from one Riemann sheet to another. The whole trajectory of a light ray in Riemann surfaces looks like a “spiral” curve. Its conformal image in $x-y$ space is the red sinelike curve in Fig. 1(d). Different Riemann sheets in Fig. 1(c) are mapped to different ribbonlike regions bounded by blue dashed lines in Fig. 1(d).

So far we have constructed a conformal lens (or a Mikaelian lens) in Fig. 1(d) by CTO from a Maxwell's fish-eye lens. Now we will employ a practical experimental system to demonstrate its properties. In the original work of optical conformal mapping, an isotropic medium with a nonuniform refractive index profile was used [4]. Here we propose a new way to visualize CTO by using a gradient-index micro-structured optical waveguide at optical frequencies (Supplemental Material, Sec. II [50]). As a specific example, we fabricate a Mikaelian lens in a structured waveguide, which is built on an air-PMMA-Ag-SiO₂ multilayer structure [Fig. 2(a)]. A laser beam of a large spot size is coupled to the waveguide through a grating, and used as a broad incident beam for a Mikaelian lens. Such a beam is denoted in red in Fig. 2(a) to show its self-focusing property in the geometric-optics limit. In Fig. 2(b) we show the effective refractive index of the constructed lens as a red curve (see Sec. III in the Supplemental Material [50]). The

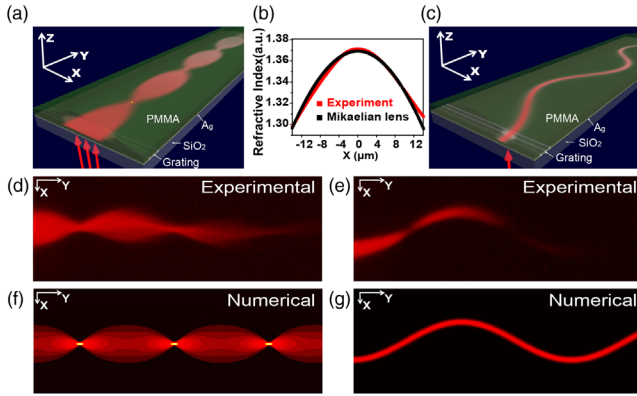


FIG. 2. Schematics and optical measurements of light rays in a conformal waveguide. (a),(c) Schematic view of the microstructured optical waveguide. (b) The effective refractive index calculated from the waveguide thickness profile (see Supplemental Material Sec. III for more details [50]). (d),(f),(e),(g) The experiment results and numerical simulations of the self-focusing effect (d),(f) and sinelike rays (e),(g) in the conformal lens.

black curve is the fitted result with the refractive index profile given by Eq. (2), designed from the conformal mapping shown in Fig. 1(b). Such a lens can be viewed as a Mikaelian lens. As theory proposed in Fig. 1(b), we observed self-focusing in our experiment (see Sec. IV in the Supplemental Material [50]) [Fig. 2(d)]. Its focusing length is a quarter of the periodicity L . Figure 2(f) depicts a numerical simulation with parameters extracted from the experiment (see Sec. V in the Supplemental Material [50]), the experiment and numerical results are in good agreement with each other. In another experiment [Fig. 2(c)], we use a laser of a small spot size to excite the waveguide and generate a narrow light ray (shown in red). Based on the theory proposed in Fig. 1(d), we also schematically show sinelike rays in the constructed lens. Figures 2(e) and 2(g) show the experimental and numerical result of light-ray trajectories, respectively, which agree very well with the theory. However, there is some absorption in experiment given in Fig. 2(e), mostly caused by fluorescence emission by rare-earth ions excited by the laser beam. This fluorescence emission is just an experimental technique used to measure the light trajectory inside the conformal waveguide (see Supplemental Material Sec. II for more details [50]), which is not necessary for the device. The absorption can be reduced by removing the rare earth ion in a practical application. In this lens, the width is about $30 \mu\text{m}$, which is about 65 times the working wavelength ($0.46 \mu\text{m}$), meaning that the device size is much larger than the wavelength.

The above experiment only demonstrates CTO in the geometric-optics limit from the self-focusing property of a Mikaelian lens in a gradient-index microstructured optical waveguide. Recently, CTO has also been expanded to wave optics [3,21–31], which enriches its application. In our other experiment, by redesigning the coupling grating in

the same waveguide structure, we achieve a conformal Talbot effect [Fig. 3(c)]. This is an important and interesting effect in wave optics and shows a big difference from the ordinary Talbot effect in a homogeneous medium. For comparison, Figure 3(a) depicts an ordinary Talbot effect with an infinite periodic incident source, where the periodic source pattern repeats along the propagation direction at integer multiples of the primary Talbot length of $2D^2/\lambda$ and is equally spaced along in the transverse direction. In a real practical system, the incident wave cannot be infinitely large. Figure 3(b) shows the results of an ordinary Talbot effect with finite periodic source. It is obvious that, for a finite source, the Talbot effect can only be maintained for a short distance due to the boundary effect (see Sec. VI in the Supplemental Material [50]). As a result, a practical ordinary Talbot effect cannot transfer the field pattern

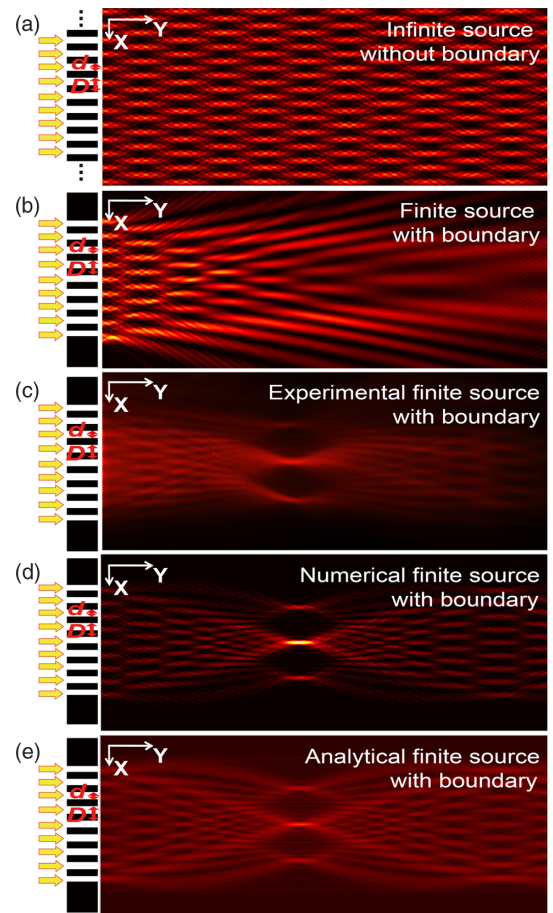


FIG. 3. Comparison between the ordinary Talbot effect and the conformal Talbot effect. (a),(b) Ordinary Talbot effect in homogeneous medium with infinite periodic source (a) and finite periodic source (b). (c),(d),(e) Self-focusing of the conformal Talbot effect in a Mikaelian lens: (c) experimental results; (d) numerical results; (e) analytical results. The figures in the left column show the schematic of the grating source, the grating period is D , the slit width is d . An incident laser is used to excite the grating source (denoted as yellow arrows).

without diffraction. However, the conformal Talbot effect in a Mikaelian lens can avoid this diffraction problem [Figs. 3(c)–3(e)]. The replicas of the finite periodic source pattern are vertically squeezed to some special positions at $y = L/4$, and the input source pattern is perfectly recovered at $y = L/2$ [Fig. 3(c)]. In comparison with the pattern illustrated in Fig. 3(b), it can be seen that the input source pattern can be transferred for a very long distance. In this process there is no diffraction loss, which happens in a finite ordinary Talbot effect [Fig. 3(b)]. The numerical simulation is given in Fig. 3(d) and analytical calculation in Fig. 3(e), which agree with the experimental results shown in Fig. 3(c). Details of the analytical solution are provided in the Supplemental Material Sec. VII [50]. In the above two experiments, we observe phenomena characteristic of both geometric optics and wave optics in the same conformal waveguide, demonstrating the capacity of CTO devices.

It is well known that information in computer science is restored and transferred as a string of bits: “0” or “1.” Here, we employ the conformal Talbot effect to transfer an encoded field pattern. By tuning the grating parameters D and d , we encode the field pattern with the two bits 0 and 1

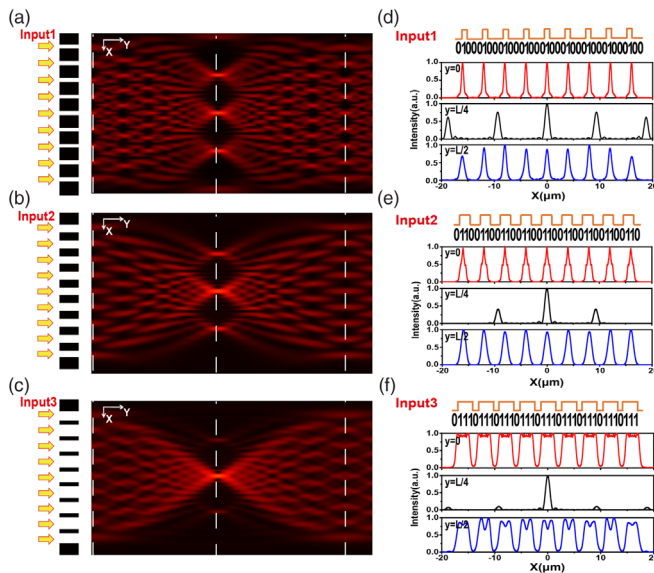


FIG. 4. Digital coding from different source sequences. (a),(b),(c) Field pattern with thirty-six bits coding sequences: (a) 0100010001000100010001000100010001000, (b) 011001100110011001100110011001100110, (c) 011101110111011101110111011101110111. The left pictures schematically show the input coding source sequences denoted by Input1, Input2, Input3. (d),(e),(f) The finite periodic coding source sequences (on top) and the normalized intensity profiles for several propagation distances. For $y = 0$, we get the input signal (red solid curve). The encoded result (black solid curve) is the field at $y = L/4$, or the focusing plane. For $y = L/2$, we get the final output result (blue solid curve), which deviates little from the input signal.

(see Supplemental Material Sec. VIII for more details [50]). Here we use thirty-six bits to investigate the digital coding information transferred through the Talbot effect in a Mikaelian lens waveguide. We find that the coding information can be transferred over a long distance with small distortion. Figures 4(a)–4(c) show that three kinds of coding sources (denoted by Input1, Input2, and Input3) can be focused and transferred in this conformal lens waveguide. Figures 4(d)–4(f) display the coding sources with specific sequences (orange line) and the normalized intensity profiles of the coding field pattern at different propagation distances. The coding sources are represented by the sequences of 0 and 1. With the coding sources (for example, Input1) imported to this conformal lens waveguide, we calculate the input field pattern at $y = 0$ [red curve in Fig. 4(d)], focusing pattern at $y = L/4$ [black curve in Fig. 4(d)], and output field pattern at $y = L/2$ [blue curve in Fig. 4(d)]. It can be clearly seen that the encoded field pattern consists of several separated peaks with specific profiles at the focusing distance, and the magnitudes of the peaks are different for different imported coding sources. Comparing the input and output patterns, we demonstrate that the coding source information could be transferred with very small distortion. Therefore, we can transfer digital coding information efficiently using the conformal Talbot effect, for instance, in an optical communication system. One could subsequently transfer this encoded signal into a normal optical chip or waveguide and use another conformal lens at the receiving port to decode the information. Therefore, the conformal Talbot effect has potential application to digital coding transfer without information loss.

In conclusion, we have employed a new platform using a gradient-index micro-structured optical waveguide to realize conformal transformation optics devices. Based on conformal mapping theory, we designed and fabricated a conformal lens to simultaneously obtain a self-focusing effect in the geometric-optics limit and a Talbot effect in the wave-optics limit. Numerical simulations and analytical calculations confirm the experimental results, which demonstrate that such a conformal device can work both in geometric optics and wave optics. We also show that this Talbot effect can be used to transfer a digital field pattern without diffraction and has potential applications in digital coding communications.

This work was financially supported by the National Key Projects for Basic Researches of China (No. 2017YFA0205700 and No. 2017YFA0303700), the National Natural Science Foundation of China (No. 11690033, No. 61322504, No. 11621091, No. 61425018, and No. 11374151), and the Fundamental Research Funds for the Central Universities (No. 20720170015). H. Y. C. also thank the support from the faculty start-up funding of Xiamen University.

X. W. and H. Y. C. contributed equally to this work.

- *Corresponding author.
kenyon@xmu.edu.cn
- †Corresponding author.
liuhui@nju.edu.cn
- [1] A. Einstein, *Science* **84**, 506 (1936).
 [2] L. Dolin, *Izv. Vyssh. Uchebn. Zaved., Radiofiz.* **4**, 964 (1961).
 [3] J. B. Pendry, D. Schurig, and D. R. Smith, *Science* **312**, 1780 (2006).
 [4] U. Leonhardt, *Science* **312**, 1777 (2006).
 [5] V. M. Shalaev, *Science* **322**, 384 (2008).
 [6] H. Chen, C. T. Chan, and P. Sheng, *Nat. Mater.* **9**, 387 (2010).
 [7] B. Zhang, *Light Sci. Appl.* **1**, e32 (2012).
 [8] U. Leonhardt and T. G. Philbin, *New J. Phys.* **8**, 247 (2006).
 [9] D. A. Genov, S. Zhang, and X. Zhang, *Nat. Phys.* **5**, 687 (2009).
 [10] H. Chen, R.-X. Miao, and M. Li, *Opt. Express* **18**, 15183 (2010).
 [11] C. Sheng, H. Liu, Y. Wang, S. Zhu, and D. Genov, *Nat. Photonics* **7**, 902 (2013).
 [12] C. Sheng, R. Bekenstein, H. Liu, S. Zhu, and M. Segev, *Nat. Commun.* **7**, 10747 (2016).
 [13] R. Bekenstein, R. Schley, M. Mutzafi, C. Rotschild, and M. Segev, *Nat. Phys.* **11**, 872 (2015).
 [14] V. H. Schultheiss, S. Batz, and U. Peschel, *Nat. Photonics* **10**, 106 (2016).
 [15] H. Chen and C. Chan, *Appl. Phys. Lett.* **91**, 183518 (2007).
 [16] S. A. Cummer and D. Schurig, *New J. Phys.* **9**, 45 (2007).
 [17] S. Zhang, D. A. Genov, C. Sun, and X. Zhang, *Phys. Rev. Lett.* **100**, 123002 (2008).
 [18] S. Guenneau, C. Amra, and D. Veynante, *Opt. Express* **20**, 8207 (2012).
 [19] D. Schurig, J. Mock, B. Justice, S. A. Cummer, J. B. Pendry, A. Starr, and D. Smith, *Science* **314**, 977 (2006).
 [20] Q. Cheng, T. J. Cui, W. X. Jiang, and B. G. Cai, *New J. Phys.* **12**, 063006 (2010).
 [21] L. Xu and H. Chen, *Nat. Photonics* **9**, 15 (2014).
 [22] H. Chen, U. Leonhardt, and T. Tyc, *Phys. Rev. A* **83**, 055801 (2011).
 [23] H. Chen, Y. Xu, H. Li, and T. Tyc, *New J. Phys.* **15**, 093034 (2013).
 [24] H. Li, Y. Xu, and H. Chen, *J. Phys. D* **46**, 135109 (2013).
 [25] L. Xu and H. Chen, *Sci. Rep.* **4**, 6862 (2014).
 [26] L. Xu, H. Chen, T. Tyc, Y. Xie, and S. A. Cummer, *Phys. Rev. B* **93**, 041406 (2016).
 [27] Y. Kim, S.-Y. Lee, J.-W. Ryu, I. Kim, J.-H. Han, H.-S. Tae, M. Choi, and B. Min, *Nat. Photonics* **10**, 647 (2016).
 [28] Y. Luo, D. Y. Lei, S. A. Maier, and J. B. Pendry, *Phys. Rev. Lett.* **108**, 023901 (2012).
 [29] J. B. Pendry, Y. Luo, and R. Zhao, *Science* **348**, 521 (2015).
 [30] L. Yu, Z. Rongkuo, and J. B. Pendry, *Proc. Natl. Acad. Sci. U.S.A.* **111**, 18422 (2014).
 [31] M. Kraft, Y. Luo, and J. B. Pendry, *Nano Lett.* **16**, 5156 (2016).
 [32] A. Mikaelian and A. Prokhorov, *Prog. Opt.* **17**, 279 (1980).
 [33] T. Tyc, H. L. Dao, and A. J. Danner, *Phys. Rev. A* **92**, 053827 (2015).
 [34] H. F. Talbot, *Philos. Mag.* **9**, 401 (1836).
 [35] L. Rayleigh, *Philos. Mag.* **11**, 196 (1881).
 [36] A. Winkelmann, *Ann. Phys. (Berlin)* **332**, 905 (1908).
 [37] H. Weisel, *Ann. Phys. (Berlin)* **338**, 995 (1910).
 [38] M. Wolfke, *Ann. Phys. (Berlin)* **345**, 194 (1913).
 [39] J. Cowley and A. Moodie, *Proc. Phys. Soc. London Sect. B* **70**, 505 (1957).
 [40] J. Cowley and A. Moodie, *Proc. Phys. Soc. London* **76**, 378 (1960).
 [41] W. D. Montgomery, *J. Opt. Soc. Am.* **57**, 772 (1967).
 [42] A. Lohmann and D. Silva, *Opt. Commun.* **2**, 413 (1971).
 [43] G. Rogers, *J. Opt. Soc. Am.* **62**, 917 (1972).
 [44] K. Patorski, *Prog. Opt.* **27**, 1 (1989).
 [45] W. Zhao, X. Huang, and Z. Lu, *Opt. Express* **19**, 15297 (2011).
 [46] W. Zhang, C. Zhao, J. Wang, and J. Zhang, *Opt. Express* **17**, 19757 (2009).
 [47] J. Wen, Y. Zhang, and M. Xiao, *Adv. Opt. Photonics* **5**, 83 (2013).
 [48] T. Gao, E. Estrecho, G. Li, O. A. Egorov, X. Ma, K. Winkler, M. Kamp, C. Schneider, S. Hofling, A. G. Truscott, and E. A. Ostrovskaya, *Phys. Rev. Lett.* **117**, 097403 (2016).
 [49] Z. Nehari, *Conformal Mapping* (McGraw-Hill Book Company, Inc., New York MR, 1952), Vol. 13, p. 640.
 [50] See Supplemental Material at <http://link.aps.org/supplemental/10.1103/PhysRevLett.119.033902> for details on the theory of conformal transformation optics, sample fabrication, experimental measurements fittings and effective refractive index, optical measurements, numerical calculations, the boundary effect on the Talbot effect, analytical solution for the Talbot effect in Mikaelian lens waveguide, digital coding, and Refs. [51–53].
 [51] A. D. Rakić, A. B. Djurišić, J. M. Elazar, and M. L. Majewski, *Appl. Opt.* **37**, 5271 (1998).
 [52] M. Abramowitz and I. A. Stegun, *Handbook of Mathematical Functions: With Formulas, Graphs, and Mathematical Tables* (Courier Corporation, North Chelmsford, 1964), Vol. 55.
 [53] V. V. Kotlyar, A. A. Kovalev, and V. A. Soifer, *Opt. Mem. Neural. Networks* **19**, 273 (2010).
 [54] U. Leonhardt and T. Philbin, *Geometry and Light: The Science of Invisibility*. *Dover Books on Physics* (Dover Publications, Inc., Mineola, N.Y., 2012).